Contrib. Plasma Phys. **50**, No. 8, 708 – 712 (2010) / **DOI** 10.1002/ctpp.200900066

Energetic-Particle-Driven Instabilities in General Toroidal Configurations

D. A. Spong[*1], **B. N. Breizman**[2], **D. L. Brower**[3], **E. D'Azevedo**[1], **C. B. Deng**[3], **A. Konies**[4], **Y. Todo**[5], and **K. Toi**[5]

[1] Oak Ridge National Laboratory, Oak Ridge, Tennessee, U.S.A.
[2] Institute for Fusion Studies, The University of Texas, Austin, Texas, USA
[3] Department of Physics, University of California, Los Angeles, CA, USA
[4] Max-Planck Institut für Plasmaphysik, EURATOM-Association, Greifswald, Germany
[5] National Institute for Fusion Science, Japan

Received 15 December 2009, revised 8 January 2010, accepted 11 January 2010
Published online 21 July 2010

Key words Energetic particles, Alfvén eigenmodes, stellarator, toroidal plasmas, three-dimensional effects.

Energetic-particle driven instabilities have been extensively observed in both tokamaks and stellarators. In order for such devices to ultimately succeed as D-T fusion reactors, the super-Alfvénic 3.5 Mev fusion-produced alpha particles must be sufficiently well confined. This requires the evaluation of losses from classical collisional transport processes as well as from energetic particle-driven instabilities. An important group of instabilities in this context are the discrete shear Alfvén modes, which can readily be destabilized by energetic particles (with velocities of the order of $v_{\mathrm{Alfvén}}$) through wave-particle resonances. While these modes in three-dimensional systems have many similarities to those in tokamaks, the detailed implementation of modeling tools has required development of new methods. Recent efforts in this direction will be described here, with an emphasis on reduced models.

1 Introduction

An improved understanding of energetic particle driven instabilities in three-dimensional systems is motivated both by the difficulties they may cause as well as opportunities that may be associated with these instabilities. In the former are concerns about first wall damage, the negative impact of enhanced fast ion losses on heating efficiency [1] and thermal plasma confinement. Under the topic of opportunities are the potential for new ways of inferring diagnostic information via MHD spectroscopy [2] (e.g., ι profile, fast ion density profile), Alfvén mode driven transport barriers [3], bootstrap current profile shaping, possibilities for stellarator shape optimization [4] of Alfvén instabilities, selective excitation of modes for ash removal, and alpha channeling for direct ion heating [5]. All of these areas will require development and experimental validation of improved modeling capabilities, ranging from rapidly applied reduced models to more comprehensive first principles calculations. This paper will describe the physics components that are necessary to understand the frequency spectrum, mode structure and stability of energetic particle-driven Alfvén instabilities in three-dimensional equilibria. These tools will be illustrated through applications to several stellarator configurations

2 Alfvén-Sound continua

The existence of Alfvén modes possessing a global mode structure in toroidal systems can be attributed to the poloidal (tokamak) and toroidal (stellarator + rippled tokamak) spatial variations in the equilibrium magnetic field. In the case of a straight cylindrical plasma with uniform magnetic field, the Alfvén spectrum is degenerate, as a result of the crossing of the adjacent continuum ($\omega^2 = k_\parallel^2 v_A^2$) lines. Variations of the magnetic field within flux surfaces remove this degeneracy and create frequency gaps at locations where the continua would have

* Corresponding author: E-mail: spongda@ornl.gov

intersected in the cylindrical limit. The first step in identifying experimentally observed Alfvén modes is the correlation of measured frequencies with these gaps. A number of models have been developed for the calculation of such continua in stellarators [6–8] and generally provide reasonable agreement with frequency lines that are measured in experiments, to within uncertainties related to imprecise knowledge of the ι- and density profiles, average ion mass and Doppler shifts related to plasma flows.

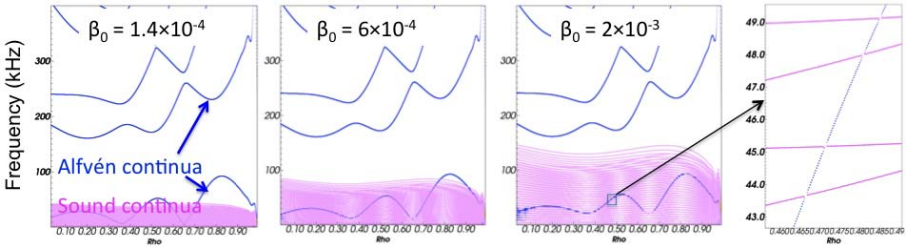

Fig. 1 Coupled Alfvén-sound continua with increasing β for n = 1 modes in LHD. Pink curves are dominated by acoustic (sound) couplings while blue curves are Alfvén dominated. Far right-hand figure is a magnification of the β = 0.002 case showing small Alfvén-sound induced gaps. (Color figure: www.cpp-journal.org).

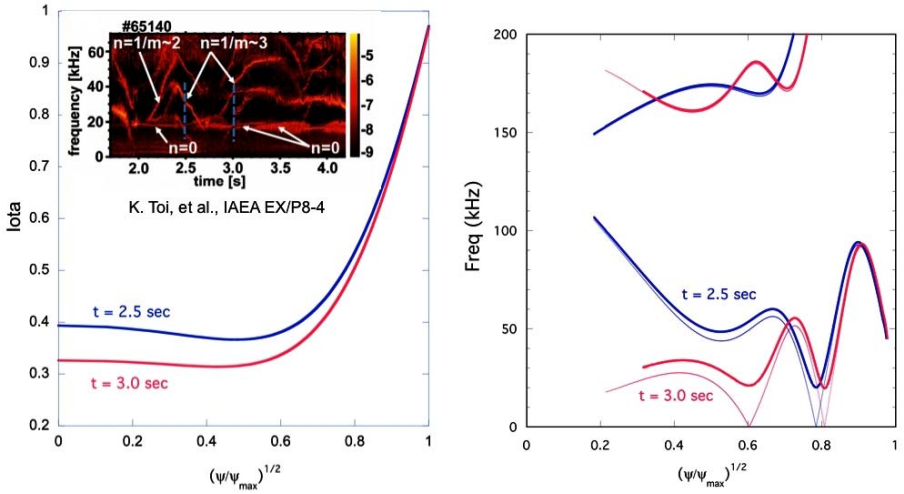

Fig. 2 (a) Reversed shear rotational transform profiles for two times in LHD RSAE discharge (inset shows measured frequency spectrogram); (b) associated n = 1 shear Alfvén only continua (lighter lines) and coupled Alfvén-sound continua (bolder lines). (Color figure: www.cpp-journal.org).

A topic of recent interest both for tokamaks [9, 10] and stellarators [4, 6, 8, 11] has been the inclusion of sound wave couplings to the shear Alfvén continua. In a three-dimensional system these couplings might be expected to become of importance when $k^2_{\|m,n}v^2_A \approx k^2_{\|m\pm\Delta m,n\pm\Delta n}C^2_s$ where Δm, Δn are the coupling intervals in the poloidal and toroidal mode numbers, $v_A = \left(B^2/\mu_0 n_{ion} m_{ion}\right)^{1/2}$is the Alfvén velocity and $C_s = \left[\Gamma\left(Z\,T_{electron} + T_{ion}\right)/m_{ion}\right]^{1/2}$is the sound speed. Here μ_0 = 4$\pi\times$ 10^{-7}H/m, n_{ion} = ion density, m_{ion} ion mass, $T_{electron,ion}$ = electron/ion temperatures, Γ = adiabatic index, and Z = ion charge state. Normally, the small size of $C^2_s/v^2_A = 0.5\Gamma\, Z\,\beta_{electron}$ might be expected to minimize such couplings. However, due to differences in magnitude between the coupled $k'_\| s$ (especially in the case of stellarators where $\Delta n = jN_{fp};\ j = 1, 2, ...;\ N_{fp}$ =field period) the Alfvén and sound continua can become coupled even at moderate values of $\beta_{electron}$. An example of the overlapping of the sound continua with the Alfvén continua as $\beta_{electron}$ is increased for an LHD discharge is illustrated in Fig. 1 based on using the STELLGAP model [7] with acoustic couplings included.

For simplicity, the plots in this figure show only the n = 1 mode continua. Inclusion of Alfvén-sound coupling effects in these continua introduces several new effects. One is the existence of new gaps where the Alfvén and

sound continua intersect (these are present on a fine-scale in the case of Fig. 1). A second is the presence of a finite frequency minimum in the coupled continua. The latter effect is illustrated in Fig. 2 for several time slices in an LHD discharge [12] where a local minimum was present in the ι profile. In this plot, couplings to the acoustic mode have been included, but the sound continua have been removed for clarity. The minima in the coupled Alfvén-sound continua of Fig. 2(b) generally agree with the frequency minima measured experimentally. Alfvén-sound couplings can introduce new eigenmodes near the minima of these continua, such as the BAAE [10, 11] (beta-induced Alfvén-acoustic eigenmode) and EGAM [13] (energetic-particle-induced geodesic acoustic mode).

Sound wave coupling effects have also been studied in the HSX stellarator experiment [14]. In this device coupled sound-Alfvén modes were initially suspected. However, systematic experimental variation of the rotational transform profile indicated that the observed frequencies were insensitive to changes in ι. This led to the conclusion that the ECH-produced electron tail predominantly excited sound waves with only weak Alfvénic couplings [14]. In Fig. 3 a sequence of n = 1 coupled Alfvén-sound continua are shown for HSX equilibria with increasing ι. The ι variation causes frequency up-shifts in the central m = 1, n = 1 Alfvén-sound gap to a greater degree than was observed in the experimental frequency lines, suggesting that the observed modes were at least not associated with this particular gap. As reported in ref. [14], sound waves existing in the m,n = 5,1 and 7,1 continua (large dots in Fig. 3) were consistent with the measured frequencies (dashed lines in Fig. 3) and their scalings. The question remains as to why these specific modes, out of the available multitude of sound and Alfvén waves were destabilized. In order to understand this both the drive (from the energetic electron tail) and damping mechanisms (continuum, e,i Landau, etc.) will need to be evaluated for the different modes in this frequency range; also, other mechanisms, such as non-ideal effects (resistivity, viscosity) and sheared plasma flows could influence the structure of these continua. These remain topics for future research.

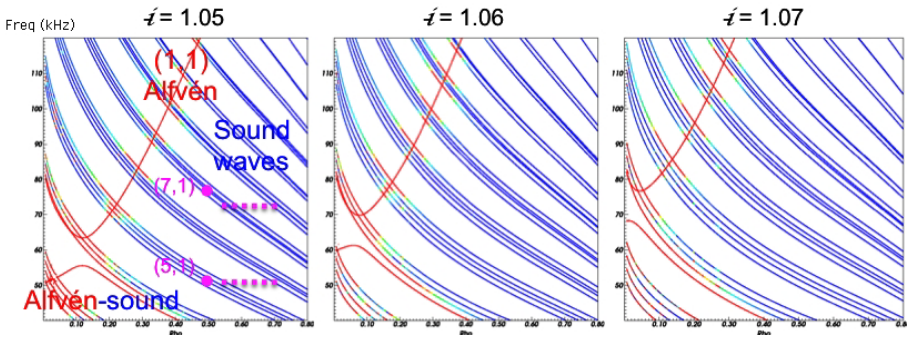

Fig. 3 Variation of n = 1 coupled Alfvén-sound continua in HSX with central value of rotational transform. Color-coding is used to indicate the strength of the sound vs. Alfvén components. Magenta dashed lines indicate the experimental frequencies, which were not observed to change significantly with variation in ι. (Color figure: www.cpp-journal.org).

3 Alfvén eigenmodes in stellarators

The next step in the analysis of Alfvén modes is the calculation of the eigenmode structures. These are the eigenmodes of the ideal MHD operator. Such an approximation is appropriate for modes that are weakly driven and near marginal stability. For this paper results from the AE3D code [15] are used, which is based on a low β, reduced MHD model, and currently does not include acoustic couplings. An efficient, solution technique has recently been developed [15] that provides eigenmodes clustered about a user specified frequency; this simplifies the process of sorting out modes that are likely to be more readily de-stabilized (i.e., less affected by continuum damping). The targeted frequencies are likely to be readily known either from experimental measurements or from the location of open gap regions in the calculated continua. An example of such an eigenmode calculation for the NCSX compact stellarator [16] is shown in Fig. 4. This is an HAE (helical Alfvén eigenmode) with strong poloidal and toroidal couplings. The continuum plot given on the left also shows evidence of continuum-crossing gap structures [17], which are often present in the continua of three-dimensional systems.

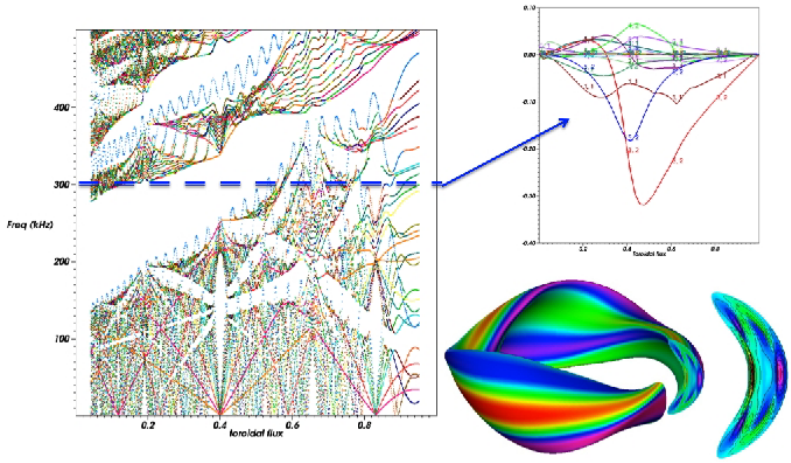

Fig. 4 (a) Strongly coupled n = 1 mode family continua (left figure) for NCSX compact stellarator; (b) example of an HAE eigenmode with global radial structure (upper right figure); (c) three dimensional mode structure in potential function (lower right figure). (Color figure: www.cpp-journal.org).

4 Stability analysis using a wave-particle energy transfer method

The linear stability of Alfvén modes in stellarators has been addressed by both continuum kinetic calculations [18] and more recently [19] using particle based methods. Due to the large deviations of trapped and transitional particle populations in some stellarators, finite orbit width effects (FOW) are expected to be of significance since they allow energetic particles to sample the Alfvén mode structure over a larger radial width than if they were confined close to fixed flux surfaces. These effects have been analyzed previously using kinetic [20] methods. In order to address these issues using particles, a technique [19] has been developed that evaluates the stability of a fixed, oscillating Alfvén mode by tracking the accumulated wave-particle energy transfers between the wave and a large collection of test particles. This method has been successfully benchmarked against a tokamak case for which results are available from other codes. Several example applications to stellarators have been made; Fig. 4 shows results from one such application to the LHD configuration. This was for a case (not an experimental discharge) where the ion density was chosen to align the n = -1 gaps in radius, resulting in a rather global m, n = (2, -1) mode at 74.1 kHz with coupling to (1, -1) and (3, -1) sidebands. In the left-hand plot of Fig. 5 the time variation of the growth rate is plotted as the ratio of the average fast ion velocity to the Alfvén velocity is increased. A distribution function that was Maxwellian in energy and beam-like in pitch angle [i.e., $f \propto \delta(\mu/\varepsilon)$] was used here. As the plot shows, the growth rate function is initially oscillatory for several wave periods as the particle markers acquire and average over resonant perturbations from the wave. For later times the growth rate settles into a quasi-stationary state with small oscillations that are presumably related to the various particle bounce/precession/transit motions. A dual weight δf scheme has been developed that removes the fixed driving frequency of the waves. The averaged growth becomes positive (unstable) at around $< v_f > /v_A \approx 0.3$ and increases with increasing $< v_f > /v_A$. In the right-hand figure, the time-averaged growth rates are plotted vs. $< v_f > /v_A$for both a beam and an isotropic fast ion distribution, showing that they reach a maximum and then start to decrease. This drop-off is caused both by the fact that for $\langle \mathrm{v}_f \rangle > \mathrm{v}_A$ the fast ion population is moving out of Landau resonance ($\mathrm{v}_{||} = \mathrm{v}_A$) with the wave and by the increasing FOW effects at the fast ion energies associated with these parameters. The decreased growth rate for the isotropic distribution vs. the beam distribution is also related to FOW effects and the greater dispersion of particle velocities in the case of the isotropic distribution – resulting in a smaller fraction of the distribution being in resonance with the wave.

5 Conclusions

Development of the theoretical/computational techniques needed to understand energetic particle-driven instabilities in three-dimensional systems is an important component of stellarator physics and will be essential for the

projection to future stellarator fusion reactors. The basic steps in the analysis of such instabilities have been outlined here and consist of calculation of the coupled Alfvén-sound continuum (identifies frequency windows where such modes are likely), computation of eigenmode structures (useful for comparison with experiment and perturbative stability analysis), and assessment of stability, including finite orbit effects (allows mapping out unstable parameter regimes). In addition, the nonlinear evolution of such instabilities and their impact on confinement must be considered and is a topic of current research. The techniques developed for energetic particle physics in stellarators are also applicable to other three-dimensional systems, such as tokamaks with symmetry-breaking effects [4] and self-organized helical states in reversed field pinches [21].

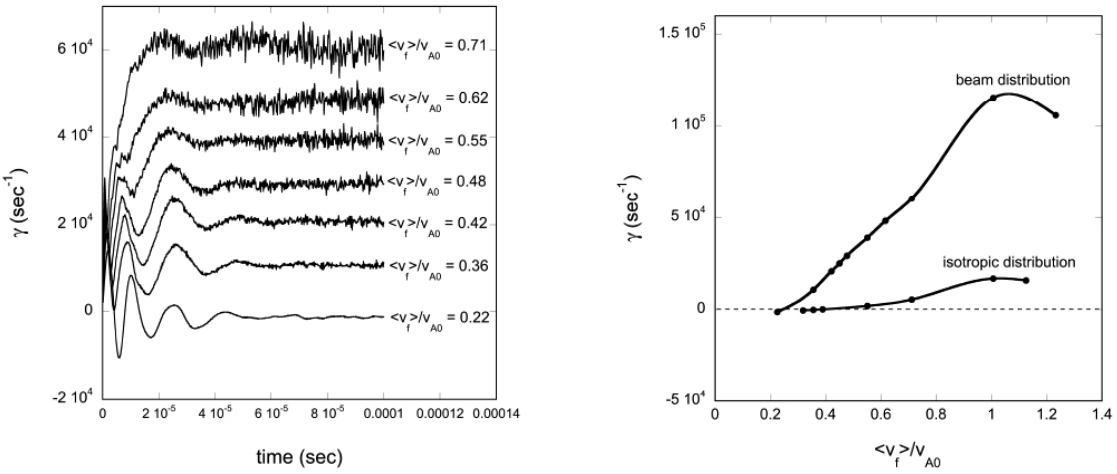

Fig. 5 (a) Time evolution of linear TAE growth rate for n = -1 mode family in LHD as a function of $< v_f > /v_A$; (b) Dependence of time-averaged growth rates on $< v_f > /v_A$ for beam-like and isotropic distributions.

Acknowledgements Research sponsored by the U.S. Department of Energy under Contract DE-AC05-00OR22725 with UT-Battelle, LLC.

References

[1] M. Osakabe, S. Yamamoto, K. Toi, et al., Nucl. Fusion **46**, S911 (2006).
[2] S.E. Sharapov, D. Testa, B. Alper, et al., Physics Letters A, Vol. 289, 127 (2001).
[3] K. Toi, M. Isobe, K. Osakabe, D. Spong, et al., Contributions in Plasma Phys. **50** 6-8, DOI 10.1002/ctpp.200900044 (2010).
[4] D.A. Spong, Y. Todo, L.A. Berry, et al. , paper TH/3-4, 22nd IAEA Fusion Energy Conference, Geneva, Switzerland (Oct., 2008).
[5] A.I. Zhmoginov, N.J. Fisch, Phys. Plasmas **16**, 112511 (2009).
[6] O.P. Fesenyuk, Ya.I. Kolesnichenko, H. Wobig, Yu.V. Yakovenko, International Workshop "Innovative Concepts and Theory of Stellarators", Kyiv, Ukraine, 28-31 May 2001, Kyiv, ISSN 1606-6723, p. 105 (2001).
[7] D. A. Spong, R. Sanchez, A. Weller, Phys. of Plasmas **10**, 3217 (2003).
[8] A. Könies, D. Eremin, Phys. of Plasmas **17**, 012107 (2010).
[9] B.N. Breizman, M.S. Pekker, S.E. Sharapov, Phys. of Plasmas **12**, 112506 (2005).
[10] N.N. Gorelenkov, H.L. Berk, E. Fredrickson, et al., Phys. Lett. A **370**, 70 (2007).
[11] D. Eremin, A. Könies, Phys. of Plasmas Phys. of Plasmas **17**, 012108 (2010).
[12] K. Toi, M. Isobe, M. Osakabe, et al., Fusion Science and Technology, LHD Special issue, to be published (2010).
[13] G.Y. Fu, Phys. Rev. Lett. **101**, 185002 (2008).
[14] C. Deng, D.L. Brower, B.N. Breizman, D.A. Spong, et al., Phys. Rev. Lett. **103**, 025003 (2009).
[15] D.A. Spong, E. D'Azevdo, Y. Todo, Phys. of Plasmas **17**, 022106 (2010).
[16] M.C. Zarnstorff, L.A. Berry, A. Brooks, et al., Plasma Phys. Controlled Fusion **43**, A237 (2001).
[17] Yu.V. Yakovenko, A. Weller, A. Werner, et al., Plasma Physics and Controlled Fusion **49**, 535 (2007).
[18] A. Könies, Phys. Plasmas **7**, 1139 (2000).
[19] D.A. Spong, A. Könies, conference proceedings of the 2009 11$^{\rm th}$ IAEA TM on Energetic Particles in Magnetic Confinement Systems, Kyiv, Ukraine, Sept. 21-23, 2009.
[20] Ya.I. Kolesnichenko, V.V. Lutsenko, A. Weller, et al., Nucl. Fusion **46** (2006) 753.
[21] R. Lorenzini, E. Martines, P. Piovesan, et al., Nature Physics **5**, 570 (2009).

